Matching 3D Models with Shape Distributions

Robert Osada, Thomas Funkhouser,
Bernard Chazelle, and David Dobkin
Princeton University, Princeton, NJ 08540, USA

Abstract

Measuring the similarity between 3D shapes is a fundamental problem, with applications in computer vision, molecular biology, computer graphics, and a variety of other fields. A challenging aspect of this problem is to find a suitable shape signature that can be constructed and compared quickly, while still discriminating between similar and dissimilar shapes.

In this paper, we propose and analyze a method for computing shape signatures for arbitrary (possibly degenerate) 3D polygonal models. The key idea is to represent the signature of an object as a shape distribution *sampled from a* shape function *measuring global geometric properties of an object. The primary motivation for this approach is to reduce the shape matching problem to the comparison of probability distributions, which is simpler than traditional shape matching methods that require pose registration, feature correspondence, or model fitting.*

We find that the dissimilarities between sampled distributions of simple shape functions (e.g., the distance between two random points on a surface) provide a robust method for discriminating between classes of objects (e.g., cars versus airplanes) in a moderately sized database, despite the presence of arbitrary translations, rotations, scales, mirrors, tessellations, simplifications, and model degeneracies. They can be evaluated quickly, and thus the proposed method could be applied as a pre-classifier in an object recognition system or in an interactive content-based retrieval application.

1 Introduction

Determining the similarity between 3D shapes is a fundamental task in shape-based recognition, retrieval, clustering, and classification. Its main applications have traditionally been in computer vision, mechanical engineering, and molecular biology. However, due to three recent developments, we believe that 3D model databases will become ubiquitous, and the applications of 3D shape analysis and matching will expand into a wide variety of other fields. First, improved modeling tools and scanning devices are making acquisition of 3D models easier and less expensive, creating a large supply of publically available 3D data sets (e.g., the Protein Data Bank [31]). Second, the World Wide Web is enabling access to 3D models constructed by people all over the world, providing a mechanism for wide-spread distribution of high quality 3D models (e.g., avalon.viewpoint.com). Finally, 3D graphics hardware and CPUs have become fast enough and cheap enough that 3D data can be processed and displayed quickly on desktop computers, leading to a high demand for 3D models from a wide range of sources.

Unfortunately, since most 3D file formats (VRML, 3D Studio, etc.) have been designed for visualization, they contain only geometric and appearance attributes, and usually lack semantic information that would facilitate automatic matching. Although it is possible to include meaningful structure and semantic tags in some 3D file formats (the "layer" field associated with entities in AutoCad models is a simple example), the vast majority of 3D objects available via the World Wide Web will not have them, and there are few standards regarding their use. In general, 3D models will be acquired with scanning devices, or output from geometric manipulation tools (file format conversion programs), and thus they will have only geometric and appearance information, usually completely void of structure or semantic information. Automatic shape-based matching algorithms will be useful for recognition, retrieval, clustering, and classification of 3D models in such databases.

Databases of 3D models have several new and interesting characteristics that significantly affect shape-based matching algorithms. Unlike images and range scans, 3D models do not depend on the configuration of cameras, light sources, or surrounding objects (e.g., mirrors). As a result, they do not contain reflections, shadows, occlusions, projections, or partial objects, which greatly simplifies finding matches between objects of the same type. For example, it is plausible to expect that the 3D model of a horse contains exactly four legs of roughly equal size. In contrast, any 2D image of the same horse may contain fewer than

0-7695-0853-7/01 $10.00 © 2001 IEEE

four legs (if some of the legs are occluded by tall grass), or it may contain "extra legs" appearing as the result of shadows on the barn and/or reflections in a nearby pond, or some of the legs may appear smaller than others due to perspective distortions. These problems are vexing for traditional computer vision applications, but generally absent from 3D model matching.

In other respects, representing and processing 3D models is more complicated than for sampled multimedia data. The main difficulty is that 3D surfaces rarely have simple parameterizations. Since 3D surfaces can have arbitrary topologies, many useful methods for analyzing other media (e.g., Fourier analysis) have no obvious analogs for 3D surface models. Moreover, the dimensionality is higher, which makes searches for pose registration, feature correspondences, and model parameters more difficult, while the likelihood of model degeneracies is higher. In particular, most 3D models in large databases, such as the World Wide Web, are represented by "polygon soups" – unorganized and degenerate sets of polygons. They seldom have any topology or solid modeling information; they rarely are manifold; and most are not even self-consistent. We conjecture that *almost every 3D computer graphics model available today contains missing, wrongly-oriented, intersecting, disjoint, and/or overlapping polygons*. As a few classic examples, the Utah teapot is missing its bottom, and the Stanford Bunny [38] has several holes along its base. The problem with these degenerate representations is that most interesting geometric features and shape signatures are difficult to compute, and many others are ill-defined (e.g., what is the volume of a teapot with no bottom?). Meanwhile, fixing the degeneracies in such 3D models to form a consistent solid region and manifold surface is a difficult problem [11, 29, 42], often requiring human intervention to resolve ambiguities.

In this paper, we describe and analyze a method for computing 3D shape signatures and dissimilarity measures for arbitrary objects described by possibly degenerate 3D polygonal models. The key idea is to represent the signature of an object as a *shape distribution* sampled from a *shape function* measuring global geometric properties of the object. The primary motivation for this approach is that the shape matching problem is reduced to the comparison of two probability distributions, which is a relatively simple problem when compared to the more difficult problems encountered by traditional shape matching methods, such as pose registration, parameterization, feature correspondence, and model fitting. The challenges of this approach are to select discriminating shape functions, to develop efficient methods for sampling them, and to compute the dissimilarity of probability distributions robustly. This paper presents our initial steps to address these issues. For each issue, we describe several options and present experimental evaluation of their relative performance. Overall, we find that the proposed method is not only fast and simple to implement, but it also provides useful discrimination of 3D shapes and thus is suitable as a pre-classifier for a recognition or similarity retrieval system.

The remainder of the paper is organized as follows. The next section contains a summary of related work. An overview of the proposed approach appears in Section 3, while detailed descriptions of issues and proposed solutions for implementing our approach appear in Section 4. Section 5 presents results of experiments aimed at evaluating the robustness and discrimination of shape distributions. Finally, Section 6 contains a summary of our experiences and proposes topics for future work.

2 Related Work

The problem of determining the similarity of two shapes has been well-studied in several fields. For a broad introduction to shape matching methods, please refer to any of several survey papers [2, 7, 14, 41, 44, 57]. To briefly review, prior matching methods can be classified according to their representations of shape: 2D contours, 3D surfaces, 3D volumes, structural models, or statistics.

The vast majority of work in shape matching has focused on characterizing similarity between objects in 2D images (e.g., [18, 27, 35, 43]). Unfortunately, most 2D methods do not extend directly to 3D model matching. The main problem is boundary parameterization. Although the 1D boundary contours of 2D shapes have a natural arc length parameterization, 3D surfaces of arbitrary genus do not. As a result, common representations of 2D contours for shape matching, such as Fourier descriptors [5], turning functions [6], bending energy functions [60], arch height functions [40], and size functions [55, 56], have no analogs for 3D models.

Shape matching has also been well-studied for 3D objects. For instance, representations for registering and matching 3D surfaces include Extended Gaussian Images [32], Spherical Attribute Images [20, 21], Harmonic Shape Images [61], and Spin Images [36]. Unfortunately, these previous methods usually assume that a topologically valid surface mesh or an explicit volume is available for every object. In addition, volumetric dissimilarity measures based on wavelets [28] or Earth Mover's Distance [48] usually rely upon a priori registration of objects' coordinate systems, which is difficult to achieve automatically and robustly. Geometric hashing [39] is a potential solution, but it requires a large amount of storage for complex models.

Another popular approach to shape analysis and matching is based on comparing high-level representations of shape. For instance, model-based approaches first decompose a 3D object into a set of features (or parts), and then compute a dissimilarity measure between ob-

jects based on the differences between their features and/or their spatial relationships. Example representations of this type include generalized cylinders [16], superquadrics [52], geons [59], deformable regions [12], shock graphs [50], medial axes [10], and skeletons [17, 24]. These methods work best when 3D models can be segmented into a canonical set of features naturally and correspondences can be found between features robustly. Unfortunately, these tasks are difficult and not always well-defined for arbitrary 3D polygonal models (e.g., what is the canonical skeleton for an unconnected set of polygons?). Moreover, feature detection and segmentation algorithms tend to be sensitive to small perturbations to the model, placing undue burden on subsequent feature correspondence and dissimilarity computation steps. Finally, the combinatorial complexity of finding correspondences in large discrete models usually leads to long computation times and/or large storage requirements.

Finally, shapes have been compared on the basis of their statistical properties. The simplest approach of this type is to evaluate distances between feature vectors [22] in a multidimensional space where the axes encode global geometric properties, such as circularity, eccentricity, or algebraic moments [45, 53]. Other methods have compared discrete histograms of geometric statistics. For example, Thacker et al [1, 4, 8, 9, 25, 26, 47, 54], Huet et al. [33], and Ikeuchi et al. [34] have all represented shapes in 2D images by histograms of angles and distances between pairs of 2D line segments. For 3D shapes, Ankerst et al. [3] has used shape histograms decomposing shells and sectors around a model's centroid. Besl [13] has considered histograms of the crease angle for all edges in a 3D triangular mesh. Besl's method is the most similar to our approach. However, it works only for manifold meshes, it is sensitive to cracks in the models and small perturbations to the vertices, and it is not invariant under changes to mesh tessellation. Moreover, the histogram of crease angles does not always match our intuitive notion of rigid shape. For example, adding any extra arm to a human body results in the same change to a crease angle histogram, no matter whether the new arm extends from the body's shoulder or the top of its head.

To summarize, many previous approaches have difficulty with 3D polygon soups because they invariably require a solution to at least one of the following difficult problems: reconstruction, parameterization, registration, or correspondence. The motivation behind our work is to develop a fast, simple, and robust method for matching 3D polygonal models without solving these problems.

3 Overview of Approach

Our approach is to represent the shape signature for a 3D model as a probability distribution sampled from a *shape function* measuring geometric properties of the 3D model. We call this generalization of geometric histograms a *shape distribution*. For example, one such shape distribution, which we call *D2*, represents the distribution of Euclidean distances between pairs of randomly selected points on the surface of a 3D model. Samples from this distribution can be computed quickly and easily, while our hypothesis is that the distribution describes the overall shape of the represented object. Once we have computed the shape distributions for two objects, the dissimilarity between the objects can be evaluated using any metric that measures distance between distributions (e.g., L_N norm), possibly with a normalization step for matching scales.

The key idea is to transform an arbitrary 3D model into a parameterized function that can be compared with others easily. In our case, the domain of the shape function provides the parameterization (e.g., the $D2$ shape distribution is a 1D function parameterized by distance), and random sampling provides the transformation.

The primary advantage of this approach is its simplicity. The shape matching problem is reduced to sampling, normalization, and comparison of probability distributions, which are relatively simple tasks when compared to prior methods that require reconstructing a solid object or manifold surface from degenerate 3D data, registering pose transformations, finding feature correspondences, or fitting high-level models. Our approach works directly on the original polygons of a 3D model, making few assumptions about their organization, and thus it can be used for similarity queries in a wide variety of databases, including ones containing degenerate 3D models, such as those currently available on the World Wide Web.

In spite of its simplicity, we expect that our approach is able to discriminate whole objects with different gross shapes rather effectively (results of experiments testing this hypothesis are presented in Section 5). In addition, it has several properties desirable for similarity matching:

- **Invariance:** shape distributions have all the transformation invariance properties of the sampled shape function. For instance, the *D2* shape function yields invariance under rigid motions and mirror imaging. In this case, invariance under scaling can be added by normalization of shape distributions before comparing them and/or by factoring out scale during the comparison. Other shape functions that measure angles or ratios between lengths are invariant to all similarity transformations.

- **Robustness:** as a bonus, random sampling ensures that shape distributions are insensitive to small perturbations. Intuitively, since every point in a 3D model contributes equally to the shape distribution, the magnitude of changes to the shape distribution are related to the magnitude of the changes to the 3D model. For

example, if a small percentage of a 3D model is perturbed (e.g., by adding random noise, by adding a small bump onto a surface, or by adding small objects arbitrarily throughout space), then a distribution of random samples from the model must also change by a small percentage. This property provides insensitivity to noise, blur, cracks, and dust in the input 3D models. We conjecture that the distributions for most global shape functions based on distances and/or angles also vary continuously and monotonically for local shape changes.

- **Metric:** the dissimilarity measure produced by our approach adopts the properties of the norm we use to compare shape distributions. In particular, if the norm is a metric, so is our dissimilarity measure. This property holds for most common norms, including L_N norms, Earth Mover's Distance, etc.

- **Efficiency:** construction of the shape distributions for a database of 3D models is generally fast and efficient. For instance, the complexity of taking S samples of the *D2* shape function from a 3D model with N triangles is $Slog(N)$. The resulting shape distributions can be approximated concisely by functions with constant complexity storage and comparison costs.

- **Generality:** shape distributions are independent of the representation, topology, or application domain of the sampled 3D models. As a result, our shape similarity method can be applied equally well to databases with 3D models stored as polygon soup, meshes, constructive solid geometry, voxels, or any other geometric representation as long as a suitable shape function can be computed from each representation. Moreover, a single database (such as the World Wide Web) can contain 3D models in a variety of different representations and file formats. Finally, shape distributions can be used in many different application domains for comparison of natural, deformable shapes (e.g., animals) and/or man-made objects (e.g., machined parts).

The interesting issues to be addressed in implementing the proposed shape matching approach are: 1) to select discriminating shape functions, 2) to construct shape functions for each 3D model efficiently, and 3) to compute a dissimilarity measure for pairs of distributions. We address these issues in the following sections. The challenge is to find methods whose combination produces a dissimilarity measure with the desirable properties listed above, while providing enough discrimination between similar and dissimilar shapes to be useful for a particular application. We propose such methods and evaluate them experimentally in Section 5 for a database of 3D polygonal models downloaded from the World Wide Web.

4 Method

In this section, we provide a detailed description of the methods we use to build shape distributions from 3D polygonal models and compute a measure of their dissimilarities.

4.1 Selecting a Shape Function

The first and most interesting issue is to select a function whose distribution provides a good signature for the shape of a 3D polygonal model. Ideally, the distribution should be invariant under similarity transformations and tessellations, and it should be insensitive to noise, cracks, tessellation, and insertion/removal of small polygons.

In general, any function could be sampled to form a shape distribution, including ones that incorporate domain-specific knowledge, visibility information (e.g., the distance between random but mutually visible points), and/or surface attributes (e.g., color, texture coordinates, normals and curvature). However, for the sake of clarity, we focus on purely geometric shape functions based on simple measurements (e.g., angles, distances, areas, and volumes). Specifically, we have experimented with the following shape functions:

- ***A3:*** Measures the angle between three random points on the surface of a 3D model.
- ***D1:*** Measures the distance between a fixed point and one random point on the surface. We use the centroid of the boundary of the model as the fixed point.
- ***D2:*** Measures the distance between two random points on the surface.
- ***D3:*** Measures the square root of the area of the triangle between three random points on the surface.
- ***D4:*** Measures the cube root of the volume of the tetrahedron between four random points on the surface.

These shape functions were chosen mostly for their simplicity and invariances. In particular, they are easy to compute and produce distributions that are invariant to rigid motions. They are invariant to tessellation of the 3D polygonal model, since points are selected randomly from the surface. They are insensitive to small perturbations due to noise, cracks, and insertion/removal of polygons, since sampling is area weighted. Finally, the $A3$ shape function is invariant to scale, while the others have to be normalized to enable comparisons.

We expect these general-purpose shape functions to be fairly distinguishing as signatures for 3D shape, as significant changes to the rigid structures in the 3D model affect the geometric relationships between points on their surfaces. For instance, consider the *D2* shape function, whose distributions are shown for a few cannonical shapes in Figure 1(a-f). *Note how each distribution is distinctive.* Also,

note how continuous changes to the 3D model affect the *D2* distributions. For instance, Figure 1(g-h) shows the distance distributions of two unit spheres as they move 0, 1, 2, 3, and 4 units apart, respectfully. In each distribution, the first hump resembles the linear distribution of a sphere, while the second hump is the cross-term of distances between the two spheres. As the spheres move farther apart, the shape distribution changes continuously.

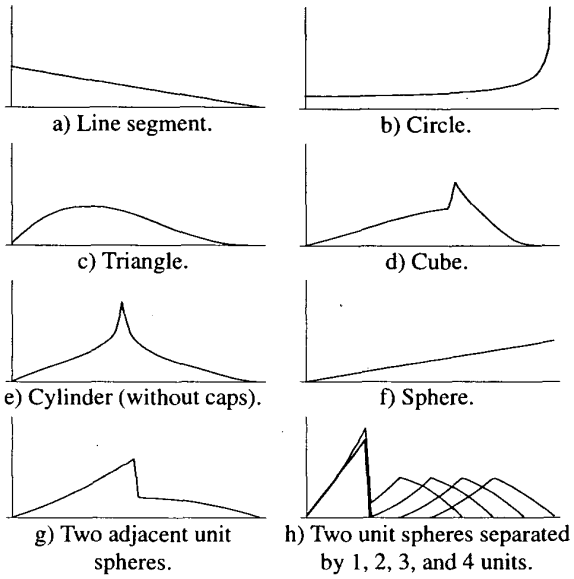

Figure 1. Example *D2* shape distributions. In each plot, the horizontal axis represents distance, and the vertical axis represents the probability of that distance between two points on the surface.

4.2 Constructing Shape Distributions

Having chosen a shape function, the next issue is to compute and store a representation of its distribution. Analytic calculation of the distribution is feasible only for certain combinations of shape functions and models (e.g., the $D2$ function for a sphere). So, in general, we employ stochastic methods. Specifically, we evaluate N samples from the shape distribution and construct a histogram by counting how many samples fall into each of B fixed sized bins. From the histogram, we reconstruct a piecewise linear function with V ($\leq B$) equally spaced vertices, which forms our representation for the shape distribution. We compute the shape distribution once for each model and store it as a sequence of V integers.

One issue we must be concerned with is sampling density. The more samples we take, the more accurately and precisely we can reconstruct the shape distribution. On the other hand, the time to sample a shape distribution is linearly proportional to the number of samples, so there is an accuracy/time tradeoff in the choice of N. Similarly, more vertices yields higher resolution distributions, while increasing the storage and comparison costs of the shape signature. In our experiments, we have chosen to err on the side of robustness, taking a large numbers of samples for each histogram bin. Empirically, we have found that $N = 1024^2$ samples, $B = 1024$ bins, and $V = 64$ vertices yields shape distributions with low enough variance and high enough resolution to be useful for the databases we've tested.

A second issue is sample generation. As our shape functions are described in terms of random points on the surface of a 3D model, we implemented the following method to generate unbiased random points with respect to the surface area of a polygonal model. First, we iterate through all polygons, splitting them into triangles as necessary. Then, for each triangle, we compute its area and store it in an array along with the cumulative area of triangles visited so far. Next, we select a triangle with probability proportional to its area by generating a random number between 0 and the total cumulative area and performing a binary search on the array of cumulative areas. For each selected triangle with vertices (A, B, C), we construct a point on its surface by generating two random numbers, r_1 and r_2, between 0 and 1, and evaluating the following equation:

$$P = (1 - \sqrt{r_1})A + \sqrt{r_1}(1 - r_2)B + \sqrt{r_1}r_2C \quad (1)$$

Intuitively, $\sqrt{r_1}$ sets the percentage from vertex A to the opposing edge, while r_2 represents the percentage along this edge (see Figure 2). Taking the square-root of r_1 gives a uniform random point with respect to surface area.

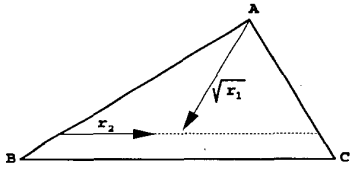

Figure 2. Sampling random point in triangle.

4.3 Comparing Shape Distributions

Having constructed the shape distributions for two 3D models, we are left with the task of comparing them to produce a dissimilarity measure. There are many standard ways of comparing two functions. Examples in-

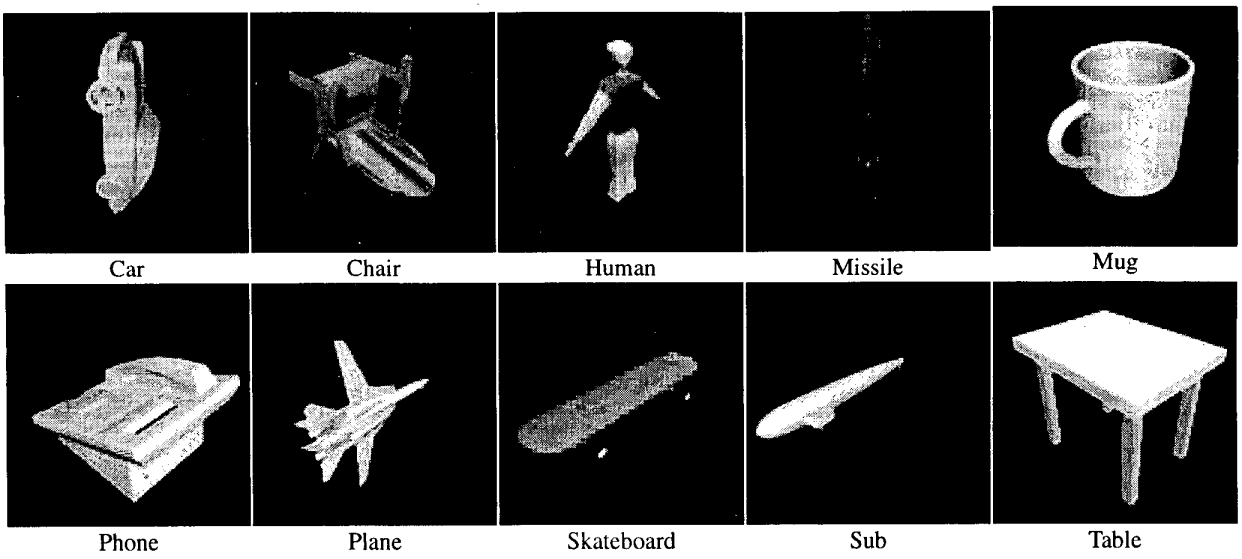

Figure 3. Images of the ten 3D models used in our initial robustness experiments.

clude the Minkowski L_N norms, Kolmogorov-Smirnov distance, Kullback-Leibler divergence distances [37], Match distances [49, 58], Earth Mover's distance [48], and Bhattacharyya distance [15]. Other methods, perhaps based on 2D curve matching, could also be used.

In our implementation, we have experimented with six simple dissimilarity measures based on L_N norms of the probability density functions (pdfs) and cumulative distribution functions (cdfs) for $N = 1, 2, \infty$.[1] In the descriptions below, assume f and g represent pdfs for two models, while $\hat{f}$ and $\hat{g}$ represent the corresponding cdfs – i.e., $\hat{f}(x) = \int_{-\infty}^{x} f$.

- **PDF L_N:** Minkowski L_N norm of the pdf: $D(f,g) = (\int |f-g|^N)^{1/N}$.
- **CDF L_N:** Minkowski L_N norm of the cdf: $D(f,g) = (\int |\hat{f}-\hat{g}|^N)^{1/N}$.

Since each shape distribution is represented as a piecewise linear function, analytic computation of these norms can be done efficiently in time proportional to the number of vertices used to store the distributions.

For certain shape functions, we must add a normalization step to the comparison process to account for differences in scale. So far, we have investigated three methods for normalization: 1) align the maximum sample values, 2) align the mean sample values, and 3) search for the scale that produce the minimal dissimilarity measure during each comparison. The first two of these can be evaluated analytically, and thus are very fast. However, they may not produce the minimal dissimilarity measures due to mismatching scales. The third method requires an optimization procedure. Specifically, if f and g represent shape distributions for two models, the minimal dissimilarity measure with normalization is then defined as:

$$\min_s D(f(x), sg(sx)) \tag{2}$$

We have implemented a simple method to perform the search over s . First, we scale our distributions so that the average sample in each distribution has value 1. Then we evaluate $D(f(x), sg(sx))$ for values of $\log s$ from -10 to 10, in 100 equally spaced intervals. We return the minimum among the results as the dissimilarity measure for the normalized shape distributions.

5 Experimental Results

The methods described in the preceding sections have been implemented in C++ and incorporated into a shape matching system that runs on Silicon Graphics and PC/Windows computers.

In order to test the effectiveness of this system, we executed a series of shape matching experiments with a database of 3D models downloaded from a variety of sites on the World Wide Web. The models comprised sets of independent polygons, without structure, adjacency information, or registered coordinate systems. The models contained anywhere from 20 to 186,000 polygons, with the av-

[1] The cdf L_1 and the cdf L_∞ norms are the L_1 Earth Mover's [48] and the Kolmogorov-Smirnov distances, respectively.

erage model containing around 7,000 polygons. Very few of the models formed a single manifold surface or even a well-defined solid region. Instead, they almost all contained cracks, self-intersections, missing polygons, one-sided surfaces, and/or double surfaces – none of which caused significant artifacts during rendering with a z-buffer, but all of which are problematic for most 3D shape matching algorithms. The experiments were run on a PC with a 400MHz Pentium II processor and 256MB of memory.

5.1 Robustness Results

In our first experiment, we tested the robustness of our dissimilarity measure to transformations and perturbations of the 3D models. Specifically, we chose ten representative 3D models (shown in Figure 3), and applied six transformations to each of them. The resulting database had seven versions of each model (the original and six transformed variants), making 70 models in all. The transformations were as follows:

- **Scale:** Grow by a factor of 10 in every dimension.
- **Rotate:** Rotate by 45 degrees three times, first around the X axis, then the Y axis, then the Z axis.
- **Mirror:** Mirror over the YZ plane, then over the XZ plane, then over the XY plane.
- **Noise:** Perturb each vertex randomly by 1% of the longest length of the model's bounding box. As vertices were not shared by adjacent polygons, this transformation introduced thin cracks (see Figure 4(a)).
- **Delete:** Randomly remove 5% of the polygons. (note the holes in the bumper and windshield in Figure 4(b)).
- **Insert:** Randomly insert copies of 5% of the polygons.

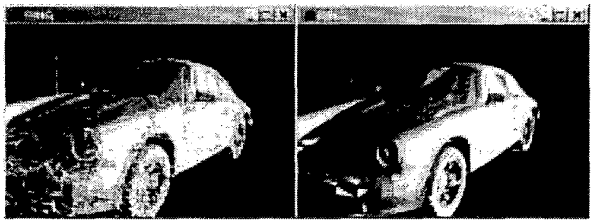

(a) 1% Noise. (b) 5% Deletion.

Figure 4. Car model after (a) perturbing vertices by 1%, or (b) deleting 5% of polygons.

We tested the robustness of our sampling method by generating the *D2* shape distribution for each model. The resulting shape distributions for all 70 models are plotted in Figure 5 (scaled to align their mean values). Note that only ten distinct curves are apparent in the plot. This is because each "thick" curve appears as the result of seven nearly overlapping shape distributions computed for different variants of the same model. For instance, the curve containing the tall spike in the middle is drawn seven times, once for each variant of the mug model. The results of this experiment demonstrate our sampling method's repeatability and its robustness to similarity transformations, noise, and small cracks and holes.

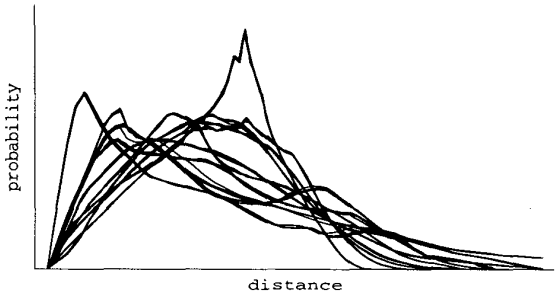

Figure 5. *D2* shape distributions for seven variants of ten models.

We further investigated the robustness of our method by testing it with different polygon tessellations of two 3D shapes. We used the Simplification Envelopes software provided by Cohen et al. [19] to produce 8 versions of the Stanford Bunny [38] ranging from 70,000 down to 600 triangles, and 6 versions of a sphere ranging from 200 down to 28 triangles. Then, we constructed *D2* shape distributions for each of these versions. The resulting 14 curves are shown in Figure 6. Note that the shape distributions vary slightly from original models to the simplified versions, but not significantly when compared to differences between the original models. This experiment corroborates our expectation that shape distributions are insensitive to changing tessellation and, more specifically, stable under model simplification.

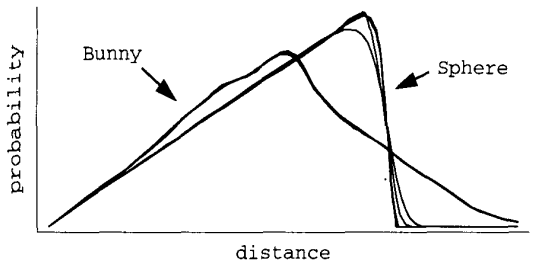

Figure 6. D2 shape distributions for tessellations of two models.

5.2 Discrimination Results

In our second experiment, we investigated the ability of our shape matching method to discriminate among similar and dissimilar shapes. As a first step towards this goal, we computed our dissimilarity measure for all pairs of the 70 shape distributions described in the previous section. During this shape matching test, the distributions were compared with the pdf L_1 norm and they were scaled by aligning their mean values. The resulting dissimilarity measures are shown as a matrix in Figure 7. In this visualization of the matrix, the lightness of each element (i, j) is proportional to the magnitude of the computed dissimilarity between models i and j. That is, each row and column represent the dissimilarity measures for a single model when compared to all other models in the database (the matrix is symmetric). Darker elements represent better matches, while lighter elements indicate worse matches. The ordering of the classes is alphabetical so one should not expect any particular darkness pattern except the clearly visible 7x7 blocks of matrix elements with indistinguishable colors. This pattern demonstrates the robustness of our distribution comparison method, as all variants of the same model produce almost the same dissimilarity measure when compared to all variants of every other model. Moreover, note the darker blocks of 7x7 matrix elements along the main diagonal. This pattern results from the fact that all 7 variants of every shape match each other better than they match any other shape. Accordingly, for this simple database, our method could be used to perfectly assign all 70 models to one of the 10 classes using a nearest neighbor classifier.

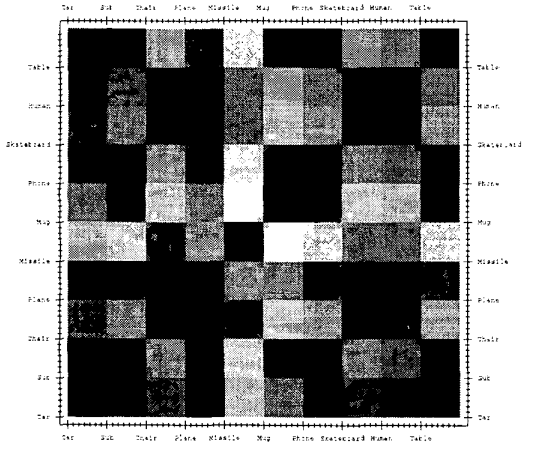

Figure 7. Similarity matrix for seven variants of ten 3D models. Lightness indicates the dissimilarity between models.

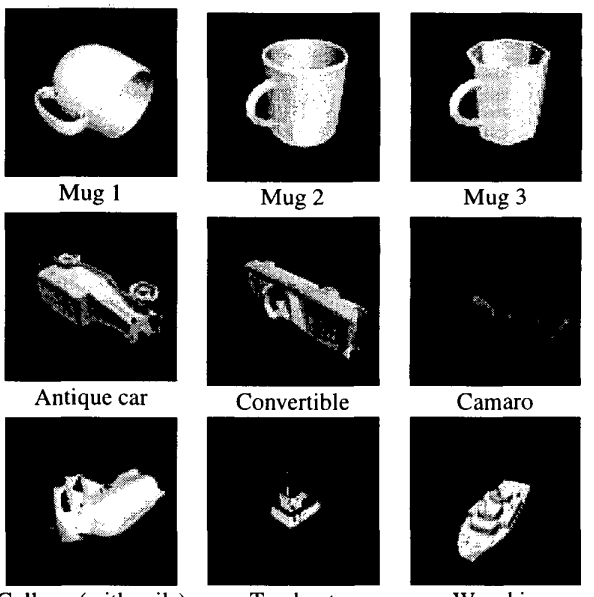

Figure 8. Example classes of shapes in our database: mugs (top row), cars (middle row), and boats (bottom row).

These initial results are encouraging, but a more interesting and challenging test is to determine how well our method can discriminate classes of shapes in a larger and more diverse database. To investigate this question, we executed a series of tests on a database of 133 models retrieved from the World Wide Web and grouped qualitatively (by function more than by shape) into 25 classes by a third party. Figure 9 summarizes the types and sizes of these classes. First, note that each class contains an arbitrary number of objects, usually determined by how many models were found in a quick search of the Web (e.g., the plane class has significantly more models than the others). Second, note that the *similarity between classes* varied greatly. For instance, some classes were very similar to one another (e.g., pens and missiles look alike), while some were quite distinct (belts). Third, note that the *similarity of objects within each class* also varied. Some classes (such as ball, mug, openbook, pen, and sub) contained 3D models with shapes greatly resembling each other, while others (such as animal, boat, car, and plane) contained models with a wide variety of shapes. This diversity within classes is shown in Figure 8, which contains pictures of three models from the mug, car, and boat classes. Note that the mugs are visually quite similar, while the cars and boats are significantly different. Another class, planes, is even more diverse, containing biplanes, fighter jets, propeller planes, and commercial jets, all similar in function, but quite different in shape.

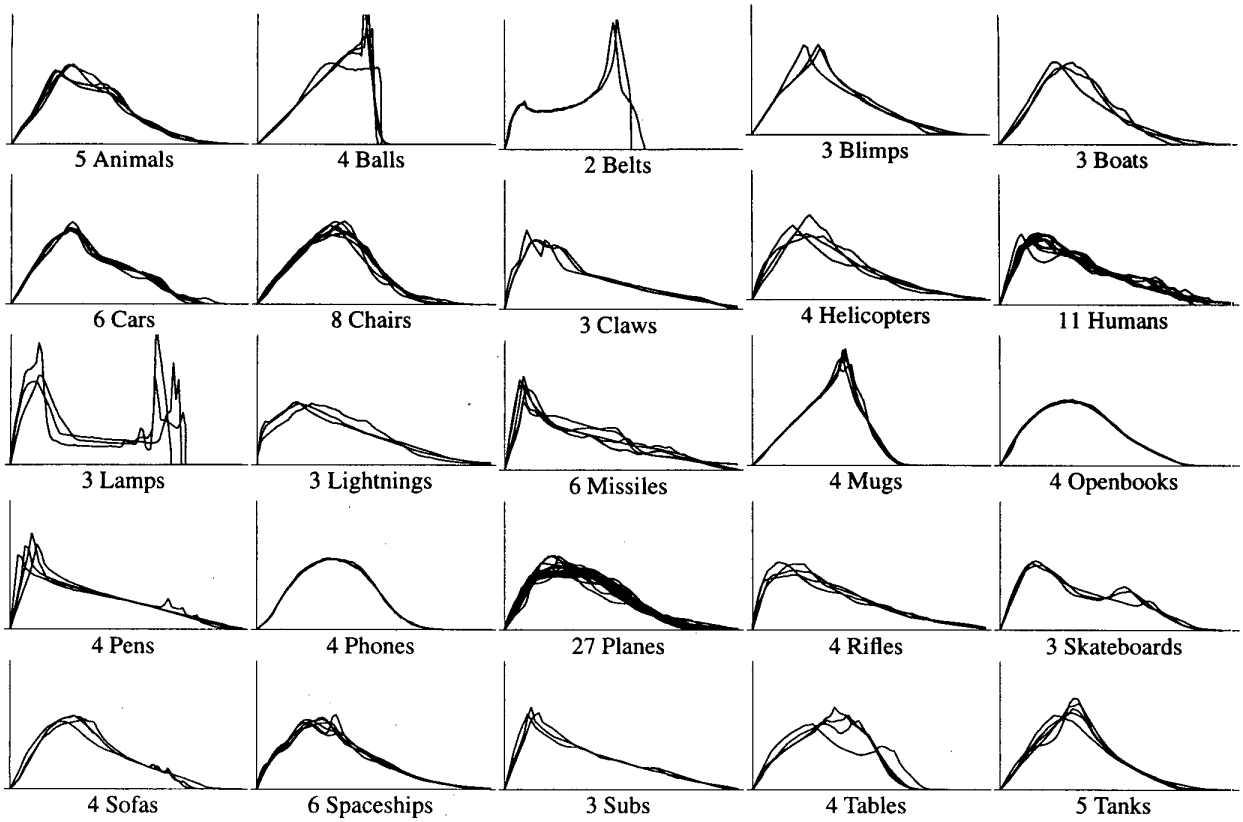

Figure 9. D2 shape distributions for 133 models grouped into 25 classes. Each plot represents a probability distribution of distance.

To investigate the ability of our shape matching methods to discriminate between classes of objects, we ran an experiment by computing the *D2* shape distributions for all 133 models. They are shown in Figure 9 – each plot shows the *D2* distribution for all 3D models of one class, normalized by their means. Examining these distributions qualitatively, we find that the shape distributions for most objects within a single class are highly correlated, as multiple curves appear almost on top of one another. Moreover, many of the classes have a distinctive shape distribution that could be used for classification. For instance, balls have a nearly linear distribution with a sharp falloff on the right, mugs have one sharp peak in the middle, belts have a peak on the right, and lamps have two large peaks with a valley in between.

To a limited degree, it is possible to infer the gross shape of some objects from their *D2* shape distributions. For instance, referring back to Figure 1, balls have a distribution resembling a sphere, belts resemble a circle, mugs resemble a cylinder, and lamps resemble two spheres separated by some distance. Although several of the other classes have visually less distinctive unimodal shape distributions, we can see that the "humps" in the distributions of different classes are usually distinguishable by their locations, heights, and shapes, leading us to believe that shape distributions could be used effectively for object classification.

To test this hypothesis and to investigate which combinations of shape functions, normalization methods, and comparison norms provided the best classification methods, we ran a series of "leave one out" classification tests. In every test, we compared the shape distribution of each model in the database (the query model) against all others. The test was repeated 90 times for all combinations of the 5 shape functions, 3 normalization methods, and 6 comparison norms described in Section 4.

Tables 1-3 contain three cross-sections of the results measured in these tests. In each table, the first column indicates the shape function, normalization method, or comparison norm used (unless otherwise specified, the *D2* shape

function, the *MEAN* normalization method, and the PDF L_1 norm was used). The second column ("First Tier") lists the percentage of top $k-1$ matches (excluding the query) from the query's class, where k is the size of the class. This criteria is stringent, since each model in the class has only one chance to be in the first tier. An ideal matching would give no false positives and return a score of 100%. The third column ("Second Tier") lists the same type of result, but for the top $2(k-1)$ matches. The fourth column lists the percentage of test in which the top match ("Nearest Neighbor") was from the query's class. Finally, the right-most column contains the computation times for sampling and comparison of shape distributions. Note that sampling times are in seconds, while comparison times are in milliseconds.

From the results in these tables, we make the following observations. First, the *D2* shape function classified objects better than the other shape functions in our tests. There are several plausible interpretations for why other shape functions proved less discriminatory than *D2*. For one, shape functions such as *D1* are difficult to represent accurately, as empirically they contain sharp peaks (e.g., the *D1* distribution for a sphere is a single delta function). For another, we noticed a trend that shape distributions for *D3* and *D4* appear similar for many types of models.

Second, in our tests, the *MAX* scaling method is not as good as *MEAN* or *SEARCH* as it suffers from the following problem. If the idealized shape density falls off near the tail, then there is a relatively high variation in the maximum sample found. Scaling the entire shape distribution based on the maximum sample affects the signature for the entire object. This result is intuitive, as the mean is a more stable statistic than the maximum. For the other normalization methods (*MEAN* and *SEARCH*) the classification results were approximately the same. We found that searching helps minimize the difference between shape distributions, but this did not improve the discriminability of the method on this database.

Third, the PDF L_1 norm performed the best for comparing shape distributions in our test. In general, the pdfs did better than the cdfs, possibly because peaks and valleys of pdf curves are easier to discriminate using L_N norms than the steep areas and plateaus of cdf curves. Meanwhile, the L_2 and L_∞ norms performed worse than the L_1 norms, in general. For higher N, the L_N norms become less forgiving of large differences, and thus perhaps our comparisons became more sensitive to outliers or normalization errors.

Finally, we examine the utility of our dissimilarity measure for classifying objects from the database with 133 models. In this test, we used the *D2* shape function, *MEAN* normalization method, and L_1 norm. Color Plate I shows the similarity matrix for this test. As in Figure 7, the lightness of each element (i, j) is proportional to the magnitude of the computed dissimilarity between models i and j (i.e., darker elements represent better matches). Thus, if the similarity metric were ideal (i.e., if it were able to read the mind of the human that formed the classes), the dissimilarity measures for models in the same class would be less (appear darker) than for ones in different classes. That is, we hope to see a sequence of darker blocks along the main diagonal, with sizes corresponding to the numbers of models in each class, with mostly lighter colors in the off-diagonal matrix elements. Given the ambiguity and diversity of the database, we believe that it would be optimistic to expect this result.

Examining the matrix shown in Color Plate I, we see that the dissimilarity values computed with our method are fairly discriminating in this test. There are many dark blocks readily apparent along the main diagonal corresponding to groups of objects within the same class that produce good matches (e.g., mugs, phones, chairs, planes, spaceships, etc.). Meanwhile, most elements off-diagonal are lighter shades, indicating relatively few false positives. Off-

Shape Function	First Tier	Second Tier	Nearest Neighbor	Sample Time (s)
A3	38%	54%	55%	12.6
D1	35%	48%	56%	8.6
D2	49%	66%	66%	8.6
D3	42%	58%	58%	13.5
D4	32%	42%	47%	15.8

Table 1. Comparison of shape functions (using *MEAN* and PDF L_1).

Scale Method	First Tier	Second Tier	Nearest Neighbor	Compare Time (ms)
MAX	41%	56%	63%	0.1
MEAN	49%	66%	66%	0.1
SEARCH	49%	66%	68%	9.0

Table 2. Comparison of normalization methods (using *D2* and PDF L_1).

Norm Method	First Tier	Second Tier	Nearest Neighbor	Compare Time (ms)
PDF L_1	49%	66%	66%	0.1
PDF L_2	47%	64%	62%	0.1
PDF L_∞	42%	59%	61%	0.1
CDF L_1	46%	63%	59%	0.2
CDF L_2	44%	63%	59%	0.1
CDF L_∞	43%	59%	57%	0.1

Table 3. Comparison of norm methods (using *D2* and *MEAN*).

diagonal blocks of dark elements often represent matches between classes (e.g., spaceship versus plane). Surprisingly, several of the classes with very diverse models (e.g., cars and planes) can be distinguished very clearly as dark blocks in this plot, indicating that our method is useful for discriminating them from other models in the database in spite of their diversity. On the other hand, there are other classes whose models did not match well in this test (e.g., boats, helicopters, etc.). Some of these failures are due to the inherent difficulties of shape matching without real world knowledge (e.g., the boats were more similar in function than shape), while others are probably due to the limitations of our implementation (e.g., L_N norms produce large dissimilarities for lamps, even though their *D2* distributions are very distinctive). Overall, for 66% of the models, our prototype system produced a top-match within the same class.

5.3 Comparison to Moments

As a final test, we compare our shape distribution method against a classifier that represents 3D models with a sequence of discrete surface moments:

$$m_{pqr} = \int_{boundary} x^p y^q z^r \, dx \, dy \, dz \qquad (3)$$

In our implementation of the moments-based classifier, the first two moments are used to register the models in a common coordinate system (as in [23]):

1. **Translation:** translate so first moments vanish.
2. **Rotation:** calculate second moments and assemble the covariance matrix. Factor the covariance matrix using Singular Value Decomposition (SVD), and orient by applying the unitary matrix of this decomposition.
3. **Scale:** scale so that the maximum eigenvalue value of the SVD is 1.

After registration, moments up to a user-specified order are calculated and stored as a shape signature. In our notation, M3 specifies that 3rd order moments and lower were used as shape descriptors (i.e., $p+q+r \leq 3$), and similarly for M4 through M7. The shape signatures are compared using a component-by-component L2 norm.

Table 4 compares the results achieved with this moment-based classifier versus the method proposed in this paper. We find that *D2* shape distributions outperform moments for classification of models in our tests. The differences are more significant for more stringent classification criteria (i.e., First-Tier) and for higher-order moments, which are known to be sensitive to noise [45]. Further studies are required to test whether *D2* shape distributions perform better than moments for larger databases or for other shape matching applications.

Method	First Tier	Second Tier	Nearest Neighbor
D2	49%	66%	66%
M3	35%	46%	63%
M4	41%	52%	64%
M5	28%	38%	55%
M6	34%	44%	54%
M7	27%	33%	51%

Table 4. Comparison of shape distributions versus moments.

6 Discussion and Conclusion

The main contribution of this paper is the idea of using random sampling to produce a continuous probability distribution to be used as a signature for 3D shape. The key feature of this approach is that it provides a framework within which arbitrary and possibly degenerate 3D models can be transformed into functions with natural parameterizations, allowing simple function comparison methods to produce robust dissimilarity metrics.

Our initial experiences verify many of the expected features of this approach. First, it is simple to implement – e.g., our whole system requires around 2000 lines of C++ code. Second, it is fast – e.g., the system takes around ten seconds to construct a shape distribution for typical 3D models containing thousands of polygons, and it computes the dissimilarity measure for any pair of shape distributions in less than a millisecond. Third, invariance and robustness properties can be ensured by choosing shape functions and norms with the desired properties – e.g., the *D2* shape function is invariant to rigid body and mirror transformations, and it is insensitive to noise, blur, cracks, tessellation, and dust in the input 3D models. Normalization of shape distributions provides invariance to scale, and using the L_N norm for comparison of distributions ensures that our dissimilarity measure is a metric.

Our experimental results demonstrate that shape distributions can be fairly effective at discriminating between groups of 3D models. Overall, we achieved 66% accuracy in our classification experiments with a diverse database of degenerate 3D models assigned to functional groups. The *D2* shape distribution was more effective than moments during our classification tests. Unfortunately, it is difficult to evaluate the quality of this result as compared to other methods, as it depends largely on the details of our test database. However, we believe that it demonstrates that our method is useful for the discrimination of 3D shapes, at least for preclassification prior to more exact similarity comparisons with more expensive methods.

An important issue for further research in 3D shape matching is development of benchmark databases containing degenerate 3D polygonal models so that different shape analysis methods can be compared. Of course, there are also many improvements that could be made to our initial prototype system in future work. For instance, one could investigate more efficient shape distribution sampling and reconstruction methods, possibly based on adaptive strategies. Or, one could also look at combining the distributions of multiple shape functions into a single classifier, or combining shape distributions with other attributes (e.g., surface colors, moments, etc.) for improved discriminability. We are currently investigating user interfaces for specifying 3D shape-based queries in an interactive retrieval system.

Another important topic for future work is to study the theoretical properties of shape distributions. For instance, it would be nice to develop a theory concerning which shape functions and norms will be good classifiers of shape. We are investigating provable properties for the *D2* shape function. Uniqueness properties for homometric *discrete* point sets (ones with the same distance distribution) have been proven by Skiena et al. [51]. They developed upper and lower bounds on the number of non-congruent homometric discrete point sets in arbitrary dimensions. Properties have also been proven for the Radon transform for a convex region C in the plane [46, 30]. This transform maps any oriented line to the length of its intersection with C. It completely specifies the region C, and it can be inverted fairly efficiently. The Radon transform has found many uses in X-ray tomography. Proving uniqueness properties for other continuous shape functions, such as *D2*, may have similar implications for reconstruction and manipulation of 3D models represented by shape distributions.

Finally, it would be interesting to investigate whether the proposed shape matching method is useful in other application domains, such as character recognition, sign-language recognition, or molecular biology.

Acknowledgements

We would like to thank Patrick Min, David Jacobs, Adam Finkelstein, and Adam's dad for their valuable discussions. Patrick also helped by assembling a bibliography on 3D shape matching, and Mao Chen retrieved the 3D models from the World Wide Web for our experiments. Thanks also go to Alfred P. Sloan Foundation for partial funding of this work.

References

[1] F. Aherne, N. Thacker, and P. Rockett. Optimal pairwise geometric histograms. *BMVC*, pages 480–490, 1997.

[2] H. Alt and L. J. Guibas. Discrete geometric shapes: Matching, interpolation, and approximation: A survey. Technical Report B 96-11, EVL-1996-142, Institute of Computer Science, Freie Universität Berlin, 1996.

[3] M. Ankerst, G. Kastenmüller, H.-P. Kriegel, and T. Seidl. Nearest neighbor classification in 3d protein databases. *ISMB*, 1999.

[4] A.P.Ashbrook, N.A.Thacker, P.I.Rockett, and C.I.Brown. Robust recognition of scaled shapes using pairwise geometric histograms. *BMVC*, pages 503–512, July 1995.

[5] K. Arbter, W. E. Snyder, H. Burkhardt, and G. Hirzinger. Application of affine-invariant fourier descriptors to recognition of 3-d objects. *IEEE Transactions on Pattern Analysis and Machine Intelligence*, 12(7):640–647, July 1990.

[6] E. M. Arkin, L. P. Chew, D. P. Huttenlocher, K. Kedem, and J. S. Mitchell. An efficiently computable metric for comparing polygonal shapes. *IEEE Transactions on Pattern Analysis and Machine Intelligence*, 13(3):209–216, March 1991.

[7] F. Arman and J. Aggarwal. Model-based object recognition in dense-range images - a review. *ACM Computing Surveys*, 25(1):5–43, 1993.

[8] A. Ashbrook, P. Rockett, and N. Thacker. Multiple shape recognition using pairwise geometric histogram based algortihms. *IEEE Image Processing*, July 1995.

[9] A. Ashbrook, N. Thacker, and P. Rockett. Pairwise geometric histograms: A scaleable solution for recognition of 2d rigid shapes. *9th SCIA*, 1:271–278, 1995.

[10] E. Bardinet, S. F. Vidal, S. D. Arroyo, G. Malandain, and N. P. de la Blanca Capilla. Structural object matching. Technical Report DECSAI-000303, Dept. of Computer Science and AI, University of Granada, Spain, February 2000.

[11] G. Barequet and S. Kumar. Repairing cad models. *IEEE Visualization '97*, pages 363–370, 1997.

[12] R. Basri, L. Costa, D. Geiger, and D. Jacobs. Determining the similarity of deformable shapes. *Vision Research*, 38:2365–2385, 1998.

[13] P. Besl. Triangles as a primary representation. *Object Recognition in Computer Vision*, LNCS 994:191–206, 1995.

[14] P. J. Besl and R. C. Jain. Three-dimensional object recognition. *Computing Surveys*, 17(1):75–145, March 1985.

[15] A. Bhattacharyya. On a measure of divergence between two statistical populations defined by their probability distributions. *Bulletin of the Calcutta Mathematics Society*, 35:99–110, 1943.

[16] T. Binford. Visual perception by computer. *IEEE Conference on Systems Science and Cybernetics*, 1971.

[17] J. Bloomenthal and C. Lim. Skeletal methods of shape manipulation. *Shape Modeling and Applications*, pages 44–47, 1999.

[18] S. Chang and J. Smith. Extracting multi-dimensional signal features for content-based visual query. *SPIE Symposium on Visual Communications and Signal Processing*, 2501(2):995–1006, May 1995.

[19] J. Cohen, A. Varshney, D. Manocha, G. Turk, H. Weber, P. Agarwal, J. Frederick P. Brooks, and W. Wright. Simplification envelopes. *Proceedings of SIGGRAPH 96*, pages 119–128, August 1996. ISBN 0-201-94800-1. Held in New Orleans, Louisiana.

[20] H. Delingette, M. Hebert, and K. Ikeuchi. Shape representation and image segmentation using deformable surfaces. *Image and vision computing*, 10(3):132–144, April 1992.

[21] H. Delingette, M. Hebert, and K. Ikeuchi. A spherical representation for the recognition of curved objects. *ICCV*, pages 103–112, 1993.

[22] R. Duda and P. Hart. *Pattern Classification and Scene Analysis*. John Wiley & Sons, New York, 1973.

[23] M. Elad, A. Tal, and S. Ar. Similarity between three-dimensional objects - an interative and interactive approach. *submitted for publication*, 2001.

[24] D. W. S. et al. Skeleton-based modeling operations on solids. *Solid Modeling*, pages 141–154, 1997.

[25] A. Evans, N. Thacker, and J. Mayhew. Pairwise representation of shape. *11th ICPR*, 1, 1992. 133-136.

[26] A. Evans, N. Thacker, and J. Mayhew. The use of geometric histograms for model-based object recognition. *4th BMVC*, pages 429–438, September 1993.

[27] M. Flickner, H. Sawhney, W. Niblack, J. Ashley, and Q. Huang. Query by image and video content: the qbic system. *IEEE Computer*, 28(9):23–32, 1995.

[28] J. Gain and J. Scott. Fast polygon mesh querying by example. SIGGRAPH Technical Sketches, 1999.

[29] A. Gueziec, G. Taubin, F. Lazarus, and W. Horn. Converting sets of polygons to manifold surfaces by cutting and stitching. *IEEE Visualization '98*, pages 383–390, 1998.

[30] S. Helgason. The radon transform. *Progress in Mathematics, Springer, 2nd ed.*, 5, 1999.

[31] L. Holm and C. Sander. Touring protein fold space with dali/fssp. *Nucleic Acids Research*, 26:316–319, 1998.

[32] B. Horn. Extended gaussian images. *Proc. of the IEEE*, 72(12):1671–1686, December 1984.

[33] B. Huet and E. Hancock. Structural indexing of infra-red images using statistical histogram comparison. *IWISP*, pages 653–656, November 1996.

[34] K. Ikeuchi, T. Shakunaga, M. Wheeler, and T. Yamazaki. Invariant histograms and deformable template matching for sar target recognition. *Computer Vision and Pattern Recognition*, 1996.

[35] C. Jacobs, A. Finkelstein, and D. Salesin. Fast multiresolution image querying. *SIGGRAPH*, pages 277–286, 1995.

[36] A. E. Johnson and M. Hebert. Using spin-images for efficient multiple model recognition in cluttered 3-d scenes. *IEEE PAMI*, 21(5):433–449, 1999.

[37] S. Kullback. *Information Theory and Statistics*. Dover, 1968.

[38] S. U. C. G. Laboratory. http://graphics.stanford.edu/data, 1996.

[39] Y. Lamdam and H. Wolfson. Geometric hashing: a general and efficient model-based recognition scheme. *ICCV*, December 1988.

[40] Y. Lin, J. Dou, and H. Wang. Contour shape description based on an arch height function. *Pattern Recognition*, 25:17–23, 1992.

[41] S. Loncaric. A survey of shape analysis techniques. *Pattern Recognition*, 31(8):983–1001, 1998.

[42] T. Murali and T. Funkhouser. Consistent solid and boundary representations from arbitrary polygonal data. *Computer Graphics (1997 SIGGRAPH Symposium on Interactive 3D Graphics)*, pages 155–162, March 1997.

[43] V. Ogle and M. Stonebraker. Chabot: Retrieval from a relational database of images. *IEEE Computer*, 28(9):40–48, 1995.

[44] A. R. Pope. Model-based object recognition: A survey of recent research. Technical Report TR-94-04, University of British Columbia, January 1994.

[45] R. J. Prokop and A. P. Reeves. A survey of moment-based techniques for unoccluded object representation and recognition. *CVGIP: Graphics Models and Image Processsing*, 54(5):438–460, 1992.

[46] A. G. Rann and A. I. Katsevich. The radon transform and local tomography. *CRC Press*, 1996.

[47] P. Riocreux, N. Thacker, and R. Yates. An analysis of pairwise geometric histograms for view-based object recognition. *BMVC*, September 1994.

[48] Y. Rubner, C. Tomasi, and L. Guibas. A metric for distributions with applications to image databases. *6th ICCV*, pages 59–66, January 1998.

[49] H. C. Shen and A. K. C. Wong. Generalized texture representation and metric. *Computer, Vision, Graphics, and Image Processing*, 23:187–206, 1983.

[50] K. Siddiqi, A. Shokoufandeh, S. J. Dickinson, and S. W. Zucker. Shock graphs and shape matching. *Computer Vision*, pages 222–229, 1998.

[51] S. Skiena, W. Smith, and P. Lemke. Reconstructing sets from interpoint distances. *Proceedings of the Sixth Annual Symposium on Computational Geometry*, pages 332–339, 1990.

[52] F. Solina and R. Bajcsy. Recovery of parametric models from range images: The case for superquadrics with global deformations. *Pattern Analysis and Machine Intelligence*, 12(2):131– 147, February 1990.

[53] G. Taubin and D. Cooper. *Geometric Invariance in Computer Vision*, chapter Object recognition based on moment (of algebraic) invariants. MIT Press, 1992.

[54] N. Thacker, P. Riocreux, and R. Yates. Assessing the completeness properties of pairwise geometric histograms. *Image and Vision Computing*, 13(5):423–429, 1995.

[55] C. Uras and A. Verri. On the recognition of the alphabet of the sign language through size functions. *IAPR*, pages 334–338, 1994.

[56] C. Uras and A. Verri. Computing size functions from edge maps. *International Journal of Computer Vision*, 23(2):169–183, 1997.

[57] R. C. Veltkamp and M. Hagedoorn. State-of-the-art in shape matching. Technical Report UU-CS-1999-27, Utrecht University, the Netherlands, 1999.

[58] M. Werman, S. Peleg, and A. Rosenfeld. A distance metric for multi-dimensional histograms. *Computer, Vision, Graphics, and Image Processing*, 32:328–336, 1985.

[59] K. Wu and M. Levine. Recovering parametrics geons from multiview range data. *CVPR*, pages 159–166, June 1994.

[60] I. Young, J. Walker, and J. Bowie. An analysis technique for biological shape. *Computer Graphics and Image Processing*, 25:357–370, 1974.

[61] D. Zhang and M. Hebert. Harmonic maps and their applications in surface matching. *IEEE Conference on Computer Vision and Pattern Recognition (CVPR '99)*, 1999.